Performance of a low-parasitic frequency domain multiplexing readout

A. E. Lowitz[1] · **A. N. Bender**[1,2] · **P. Barry**[1,2] · **T. W. Cecil**[2] · **C. L. Chang**[1,2] · **R. Divan**[3] · **M. A. Dobbs**[4] · **A. J. Gilbert**[4] · **S. E. Kuhlmann**[2] · **M. Lisovenko**[5] · **J. Montgomery**[4] · **V. Novosad**[5] · **S. Padin**[1,2] · **J. E. Pearson**[5] · **G. Wang**[2] · **V. Yefremenko**[2] · **J. Zhang**[2]

Abstract Frequency-domain multiplexing is a readout technique for transition edge sensor bolometer arrays used on modern CMB experiments. Here we present design details and performance measurements for a low-parasitic frequency domain multiplexing readout. Reduced parasitic impedance reduces crosstalk between readout channels. This allows higher multiplexing factors. Reduced parasitic resistance enables operation of lower-resistance bolometers, which enables better optimization of R_{bolo} for improved readout noise performance. The prototype system has noise performance comparable to SPT-3G readout hardware when biased above T_c. Additionally, we have demonstrated a factor of two improvement in parasitic resistance compared to SPT-3G hardware. Ongoing work seeks to further reduce parasitic impedances, leading to a laboratory demonstration of a readout with lower-resistance bolometers.

Keywords frequency domain multiplexing, transition edge sensors

1 Introduction

Frequency domain multiplexing is a technique to read out many transition edge sensor (TES) bolometers on a single pair of wires. One inductive-capacitive (LC) filter is connected to each bolometer, assigning that bolometer a unique readout and bias frequency. Signals from all of the bolometers are combined, amplified using a cryogenic amplifier (typically a SQUID array), and the individual frequencies for each bolometer are later demodulated in room temperature digital electronics. In the digital frequency domain multiplexing architecture used by SPT-3G (DfMux), 66 bolometers are read out on a single pair of wires [1]. The carrier signal, after passing through the LC filters and the TES bolometer, is inductively coupled to a series SQUID (superconducting quantum interference device) array (see Fig. 1). To maximize the effective dynamic range of the SQUID, digital active nulling (DAN) is applied

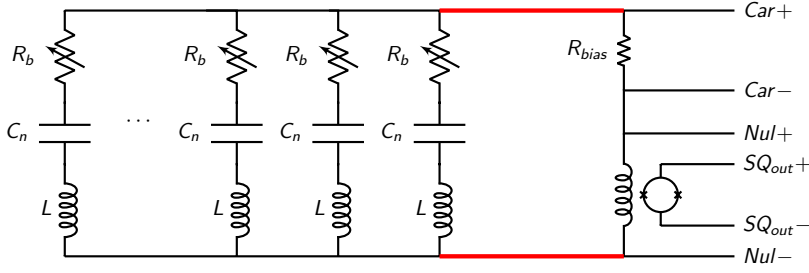[1]Kavli Institute for Cosmological Physics, University of Chicago, Chicago, IL
[2]High-Energy Physics Division, Argonne National Laboratory, Argonne, IL
[3]Center for Nanoscale Materials, Argonne National Laboratory, Argonne, IL
[4]Department of Physics, McGill University, Montreal, QC
[5]Materials Sciences Division, Argonne National Laboratory, Argonne, IL

Fig. 1 Schematic showing the cold DfMux circuit. The wiring between the LC chip and the SQUID is indicated by thicker, red lines. This wiring is a significant source of crosstalk in the cold portion of the DfMux readout, as discussed in section 2. L and C labels indicate the planar superconducting inductors and capacitors of the LC filters. The R_b labels indicate the variable resistance TES bolometers. Labels on the right side indicate the carrier ('Car', i.e. the AC bias), nuller ('Nul'), and SQUID output ('SQ$_{out}$') lines. (Color figure online.)

as a nulling signal at the SQUID input [1, 2]. This 'nuller' is the science signal. This architecture has demonstrated good on-sky performance with SPT-3G [3, 4] with multiplexing factors of up to 68x, but could benefit from improved scalability and electrical performance when applied to future ultra-large focal planes such as those for CMB-S4.

2 Motivation

In the DfMux system, the LC filters which assign a different bias and readout frequency to each bolometer are on the $\sim$250 mK stage, near the detectors. A multiplexing unit of bolometers (66 bolometers plus 2 calibration resistors in the case of SPT-3G) is called a comb. Wiring between the LC chip and the SQUID consists of broadside-coupled NbTi striplines encapsulated in Kapton and ultrasonically soldered to the LC circuit board on one end and to a breakout circuit board that connects to the SQUID circuit board on the other end [5]. The dominant source of crosstalk in the cold portion of the readout is parasitic impedance in this wiring (shown in thick, red lines in Fig. 1), which is 60 cm long to allow the SQUID chip to sit on the 4 K stage, physically and thermally distant from the LC filters. Parasitic impedance in this part of the circuit sets up a voltage divider effect such that as the resistance of any bolometer varies according to deposited optical power from the sky, the ratio of the voltage divider is modulated, changing the voltage biases supplied to all other bolometers. This causes a change in TES resistances across the comb that mimics those due to optical power deposition [6]. Stable operation of detectors requires the parasitic impedance to be small relative to the TES resistance during operation, therefore the parasitic sourced by the LC-SQUID wiring sets an effective lower limit to the resistance of any TES element. Ability to operate bolometers at lower resistances is desirable because it opens up a larger range of phase space over which R_{bolo} can be optimized to improve readout noise performance. In frequency multiplexing sytems, the optimal bolometer resistance for readout noise performance is typically in the 0.5-1.0 Ω range, a factor of 2-4 lower than SPT-3G bolometers.

The primary goal of this work is to develop a modified DfMux architecture which minimizes the parasitic impedance of the wiring between the LC filters and the SQUID. This will
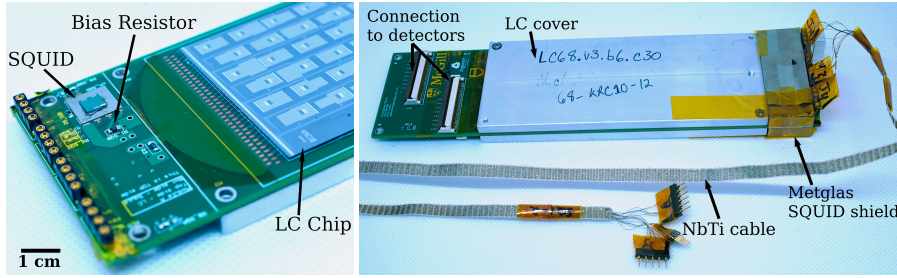
Fig. 2 *Left:* Partially-assembled prototype circuit board showing the SQUID chip, LC chip, bias resistor, and SIP connectors. Note that the wiring traces between the LC chip and the SQUID chip are made as short and as wide as possible to minimize parasitic inductance. *Right:* Fully-assembled prototype circuit board showing the Metglas cover for the SQUIDs, aluminum cover for the LC chips, and NbTi twisted pair ribbon cable which connects the board to a wiring feedthrough at 4 K. (Color figure online.)

substantially reduce crosstalk, as well as improve readout noise performance by allowing the operation of lower resistance bolometers.

3 Design

The wiring between the SQUID and the LC chip should be as short and wide as possible to reduce the parasitic impedance. One straightforward way to achieve this is to move the SQUID from the 4 K stage to the 250 mK stage, on the same circuit board as the LC chip, and to use wide wiring traces. The design of the prototype hardware retains as much of the existing DfMux design as possible. By making minimal changes, this design reaps the benefits of reduced crosstalk, reduced parasitic resistance, and improved scalability, while inheriting a relatively high level of technological maturity from the existing technology. To that end, the prototype circuit board is identical to the SPT-3G LC board from the input to the LC chip through to the connections to the detector wafer. A small extension was added to the input end of the board to accommodate the SQUID chip and its circuitry. This design minimizes the wiring length between the SQUID and LC chips, which will significantly reduce parasitics from that section of wiring. A single circuit board houses one LC chip and one SQUID chip on each side. Additionally, the extension to the board is short enough that the prototype hardware fits in every SPT-3G cryogenic testbed (and in principle, in the telescope itself) as a drop-in replacement for the standard SPT-3G DfMux readout hardware. This enables rapid and straightforward testing of the prototype architecture alongside SPT-3G hardware for comparison. Refer to Fig. 2 for photographs of the prototype circuit board design.

SQUIDs are sensitive magnetometers and require careful magnetic shielding in order to operate optimally as an amplifier. An aluminum box (for mechanical protection) covered with six layers of Metglas [7] (a high-permittivity material used for magnetic shielding), shown in Fig. 2, covers the SQUIDs. Comparison testing has shown that the Metglas box performs as well as an Ammuneal box for magnetic shielding in this application [8]. A separate aluminum cover acts as a mechanical shield for the LC chips.

A convenient additional benefit of removing the long wiring between the LC chip and the SQUID chip is that it eliminates the most complicated, expensive, and labor intensive component of the cryogenic wiring. Long wiring is still required to reach from the detector

stage to the 4 K stage. However, since the long wiring in the prototype system is between the SQUID output and the warm electronics (instead of between the SQUID and the LC), the impedance of this long wiring does not contribute to crosstalk. Therefore, the technical requirements for this wiring become trivial. The current prototype uses commercially-available NbTi twisted-pair woven loom ribbon cable, hand-connectorized with SIP (single inline package) socket connectors. Future revisions may use the same NbTi ribbon cable with commercially-potted connectors for improved scalability.

4 Performance

4.1 SQUID Performance at 250 mK

The prototype system has been tested primarily using NIST SA13 SQUID arrays. Their performance at sub-Kelvin temperatures is comparable to or slightly better than their performance at more typical operating temperatures of 2 - 4 K. Fig. 3 (*Top Left*) shows a comparison plot of the flux bias versus output voltage for a representative SA13 at three temperatures. Performance is very similar at all three temperatures, with a marginal increase in peak-to-peak voltage and transimpedance at lower temperatures.

SQUID thermal dissipation is also an important consideration when putting SQUIDs on the same thermal stage as detectors. The thermal dissipation of a SQUID can be estimated as the product of the current bias and the voltage offset at the SQUID output. Tuned at a typical operating current- and flux- bias, a single representative SA13 (able to operate one comb of bolometers) dissipates about 150 nW of heat onto the detector stage. At this level of thermal dissipation, operating small numbers of SA13s on the cold stage works well, but scaling up to the hundreds of SQUIDs required for operation of a large detector array is not feasible using a typical sorption refrigerator. For example, a Chase Cryogenics [9] gaslight sorption refrigerator provides ∼4 μW of cooling power on the ∼250 mK stage. For scalability, either a dilution refrigerator or a SQUID with lower thermal dissipation will be required.

4.2 Bolometer Operation and Noise Performance

A side-by-side measurement of the prototype and SPT-3G DfMux hardware parasitic resistance demonstrates a factor of two improvement in median parasitic resistance, as shown in Fig. 3 (*Bottom Right*). This demonstration of decreased parasitic resistance paves the way to operating lower-resistance bolometers.

Of a possible 66 bolometers per comb, 58 are operable on the test comb in our current testing configuration. The eight missing bolometers are known flaws on the detector wafer and LC chip. A network analysis (carrier signal divided by nuller signal) showing the LC resonance peaks is shown in Fig 3. The detector wafer used in all of the tests described in this work is an SPT-3G wafer that was used on-sky in 2017. When comparing the prototype to SPT-3G hardware, the SPT-3G hardware data is laboratory test data taken on the same detector wafer at the same time or nearly the same time as the prototype hardware data.

A measurement of the median noise of the prototype at $T > T_c$, an effective metric of readout-specific noise, is comparable to that of SPT-3G hardware (see Fig. 3 *Bottom Left*). This is also comparable to the full, fielded readout noise performance of the SPT-3G array [4]. Of the full comb of 58 bolometers that can be biased, we have successfully placed 57 into the TES superconducting transition to a fractional resistance of $0.2 \times R_n$ and held
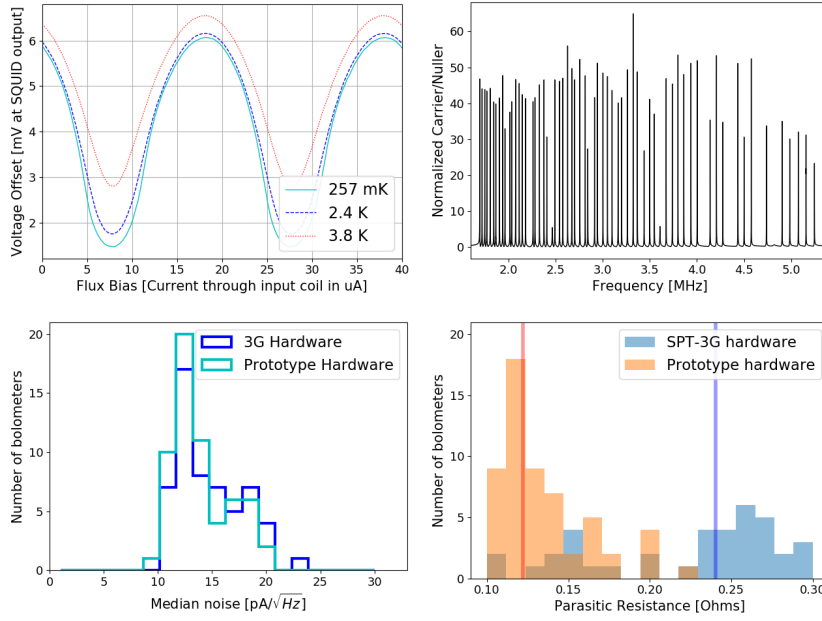
Fig. 3 *Top Left:* Performance of the NIST SA13 SQUIDs is similar across a range of temperatures. Shown here is the flux bias vs the SQUID voltage offset for the same SQUID chip at its optimal (maximal peak-to-peak voltage) current bias. For this SQUID chip, the transimpedances were $Z=945\,\Omega$, $Z=850\,\Omega$, and $Z=683\,\Omega$ at 257 mK, 2.4 K, and 3.8 K respectively. *Top Right:* Network analysis (carrier signal divided by nuller signal, across the full readout frequency range) of the prototype comb showing 61 bolometer peaks and two calibration resistor peaks (low peaks at $\sim$2.5 MHz and $\sim$3.6 MHz) *Bottom Left:* The prototype system has similar noise performance to SPT-3G readout hardware at $T > T_c$. *Bottom Right:* The reduced wiring length between the SQUID chip and LC chip substantially reduces the parasitic resistance in the prototype system compared to standard DfMux readout hardware. Shown here is the parasitic resistance of one comb of bolometers on prototype hardware and one comb on SPT-3G hardware. The orange and blue vertical lines indicate the medians for the prototype and SPT-3G hardware respectively. (Color figure online.)

them there with good stability under dark, steady-state conditions. Fig. 4 shows resistance versus power curves for a representative selection of bolometers as they are dropped into the TES superconducting transition. For comparison, under the same conditions, the standard SPT-3G readout hardware was able to operate at no lower than $0.3 \times R_n$ before the bolometers became too unstable and the whole comb latched. The improved stability at very low fractional resistances with the prototype hardware likely results from the decreased parasitic resistance in the prototype system, but more investigation is required to develop a detailed understanding of the performance improvements.

While there is not yet a detailed measurement of the parasitic inductance in the prototype system, a reasonable estimate of the likely range based on the geometry of the traces between the SQUID and the LC on the prototype circuit board is 5-10 nH. For comparison, the measured parasitic inductance between the SQUID and the LC in the SPT-3G readout system is 45 nH [5]. From these parasitic inductance values, the effect on crosstalk can be simulated. For an SPT-3G-like system with 45 nH parasitic inductance, the simulated median nearest-neighbor crosstalk is 0.58%. Reducing the parasitic inductance to 10 nH, a conser-
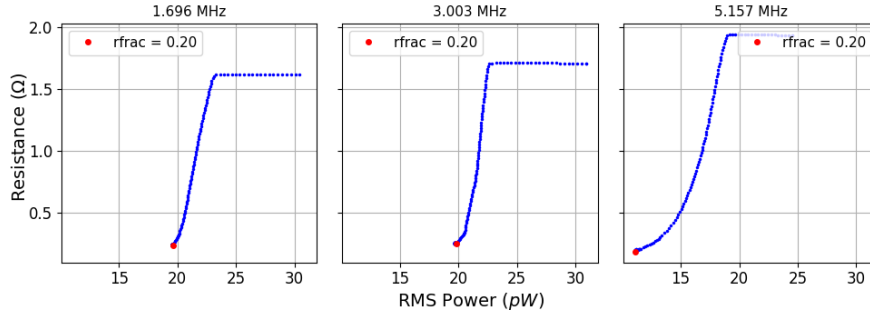
Fig. 4 Operation of a full comb of 57 bolometers down to a fractional resistance of $R_{frac} = 0.2 \times R_n$ has been demonstrated with the prototype. Shown are resistance vs power curves for three representative bolometers as they drop into the superconducting transition. Each bolometer tuning step from maximum bias power down into the superconducting transition is indicated by a small blue dot and the final tuned point is indicated by a large red dot. These curves have been corrected to remove the parasitic resistance. (Color figure online.)

vative estimate for the prototype hardware, reduces the simulated median nearest-neighbor crosstalk to 0.17%.

5 Conclusions and Future Work

In summary, we have demonstrated operation of a full comb of frequency multiplexed bolometers using the prototype hardware. Readout noise performance is comparable to that of SPT-3G hardware. NIST SA13 SQUIDs perform well overall at sub-Kelvin temperatures, however to improve scalability by enabling operation of a large number of SQUIDs on the cold stage without requiring a dilution refrigerator, SQUIDs with lower thermal dissipation will be required to operate a large number of detectors without requiring a dilution refrigerator. Finally, we have demonstrated reduction in parasitic resistance by a factor of two compared to SPT-3G readout hardware. This improvement in $R_{parasitic}$ enables operation of bolometers with lower resistance than SPT-3G, which opens up a larger range of phase space for optimizing R_{bolo} based on noise performance. Broadly, the prototype architecture shows promise as a more scalable, potentially higher-multiplexing-factor, alternative to the standard DfMux system, and more detailed characterization and laboratory testing is warranted to fully mature this technology.

In ongoing and future testing of this architecture, focus will be on detailed characterization of the in-transition noise performance and crosstalk performance of bolometers operated with the prototype hardware. Additionally, we plan to make a detailed measurement of the actual thermal dissipation of the SA13 SQUIDs in this configuration and hope to identify a SQUID model with significantly lower thermal dissipation, which will improve scalability. We also plan to test the prototype architecture with lower resistance bolometers and scale up to operating a larger number of combs.

References

1. A.N. Bender, et al. *Proc. SPIE, Millimeter, Submillimeter, and Far-Infrared Detectors and Instrumentation for Astronomy VII.* **9153**, 91531A, (2014)
2. T. de Haan, G. Smecher, and M. Dobbs. *Proc SPIE, Millimeter, Submillimeter, and Far-Infrared Detectors and Instrumentation for Astronomy VI.* **8452**, 84520E, (2012)
3. A.N. Bender, et al. *Proc. SPIE, Millimeter, Submillimeter, and Far-Infrared Detectors and Instrumentation for Astronomy IX.* **10708**, 1070803, (2018)
4. A.N. Bender, et al. *J. Low Temp. Phys.* **This Special Issue**, (2019)
5. J.S. Avva, et al. *J. Low Temp. Phys.* **193**(3-4), 547, (2018)
6. M.A. Dobbs et al. *Review of Scientific Instruments.* **83.7**, 073113, (2012)
7. Metglas, Inc., subsidiary of Hitachi Metals America, ltd, Conway, SC, metglas.com
8. A.E. Lowitz, A.N. Bender, M.A. Dobbs, and A.J. Gilbert, *Proc. SPIE, Millimeter, Submillimeter, and Far-Infrared Detectors and Instrumentation for Astronomy IX.* **10708**, 107081D, (2018)
9. Chase Research Cryogenics, Sheffield, UK, chasecryogenics.com